Accretion onto Black Holes
PHY4002W Honours Project

Anton van Niekerk*
VNKANT007
Supervisor: Dr. G. Tupper†
Department of Physics, University of Cape Town

November 3, 2009

Abstract

The accretion rates of a spherically symmetric, perfect fluid accreting onto black holes predicted by different theories are derived and the differences are investigated.

*antn.vnkrk@gmail.com
†gary.tupper@uct.ac.za

Contents

1 Introduction

Except for Einstein's general theory of relativity, there are several alternative theories of gravitation. Examples of such theories are string theory and braneworld theories. One possible way of distinguishing between the different gravitational models is by observing the accretion rate of matter onto black holes.

In this project, a perfect, spherically symmetrically test fluid accretes onto a spherically symmetric black hole. It is assumed that there is no back reaction in the accretion.

The spacetime metrics to be used in the project are:

- The Schwarzschild solution of general relativity [1]. It is the simplest solution in that it is spherically symmetric, uncharged and non-rotating. The solutions of the other cases will be compared to this one.
- The Reissner-Nordström solution for a charged, non-rotating black hole [1]. In this case the black hole will have two horizons. The extremal case (where the electric charge is large enough to merge the two horizons) corresponds to the conformal Brans-Dicke theory of a scalar field coupling to the metric. This situation emerges in certain braneworld theories [2].
- The Reissner-Nordström dilatonic case. This case describes charged black hole, also with two horizons arising from superstring theory [3].
- The Horava-Witten braneworld black hole. This case comes from M-theory in which an additional spatial dimension to the 10 spacetime dimensions already present arises. This case is interesting because the singularity has no event horizon surrounding it [4].

In the theories where there are additional spatial dimensions to the usual three, the metric used was the effective one in four spacetime dimensions. In such cases there are two possible metrics related by conformal transformations (the metrics are said to correspond to different frames). We then use the metric in which test-particle trajectories are world-lines.

2 The critical point

In this section we derive the speed of sound at the critical point of a spherically symmetric ideal test fluid, accreting on a spherically symmetric black hole, with an arbitrary metric described by the squared line-element

$$ds^2 = A(r)dt^2 - B(r)dr^2 - C(r)\left(d\theta^2 + \sin^2\theta d\phi^2\right) \tag{1}$$

2.1 Preliminary results

Under the assumption that the fluid has a stationary solution to its accretion, and that it has an energy-momentum tensor

$$T_{\mu\nu} = (\rho + p)\, U_\mu U_\nu - p g_{\mu\nu} \tag{2}$$

(where U is the fluid's four-velocity, ρ its mass-energy density and p is its pressure. $g_{\mu\nu}$ is the spacetime metric) we obtain the relativistic continuity and Euler equations, respectively:

$$U^\mu \rho_{,\mu} + (\rho + p) U^\mu{}_{;\mu} = 0 \tag{3}$$

$$U^\nu U^\mu{}_{;\nu} = \frac{(g^{\mu\nu} - U^\mu U_\nu) p_{,\nu}}{\rho + p} \tag{4}$$

Introducing some notation for convenience, we write the upper-indexed radial component of the four-velocity as

$$U^r = U \tag{5}$$

From (1) the lower-index radial component of the four-velocity will consequently be

$$U_r = g_{r\mu} U^\mu = -BU \tag{6}$$

We see that the identity

$$U_\mu U^\mu = 1 \tag{7}$$

(in the units c=G=1) is satisfied for the zeroth component

$$U^0 = \sqrt{\frac{(1 + BU^2)}{A}} \tag{8}$$

(and therefore $U_0 = \sqrt{A\,(1 + BU^2)}$).

We introduce the further notation

$$F_{,r} = F' \tag{9}$$

where F is any function function of the coordinates.

2.2 The derivation

Equations (3) and (4) lead to

$$\sqrt{ABC^2}U \exp \int \frac{d\rho}{\rho + p} = -\alpha \tag{10}$$

$$AU^0 \exp \int \frac{c_s^2 d\rho}{\rho + p} = \gamma \tag{11}$$

respectively. Here $c_s^2 = \frac{dp}{d\rho}$ is the speed of sound in the accreting fluid squared, and α and γ are positive integration constants to be determined case wise. Note that the radial velocity U of the fluid is negative, so that equation (10) has no contradiction.

Taking the logarithmic derivative of (11) with respect to r, we obtain

$$\frac{c_s^2 \rho'}{\rho + p} + \frac{U^{0\prime}}{U^0} + \frac{A'}{A} = 0 \tag{12}$$

From (8), we have

$$U^{0\prime} = \frac{A\left(B'U^2 + 2BUU'\right) - A'\left(1 + BU^2\right)}{2A\sqrt{\left(1 + BU^2\right)/A}} \tag{13}$$

and thus

$$\frac{U^{0\prime}}{U^0} = -\frac{1}{2}\frac{A'}{A} + \frac{1}{2}\frac{B'U^2 + 2BUU'}{1 + BU^2} \tag{14}$$

Substituting this in (12), we have

$$\frac{c_s^2 \rho'}{\rho + p} = -\frac{1}{2}\frac{A'}{A} - \frac{1}{2}\frac{B'U^2 + 2BUU'}{1 + BU^2} \tag{15}$$

Taking the logarithmic derivative of (10), we have

$$\frac{\rho'}{\rho + p} + \frac{\left(\sqrt{ABC^2}U\right)'}{\sqrt{ABC^2}U} = 0 \tag{16}$$

This simplifies to

$$\frac{\rho'}{\rho + p} = -\left(\frac{U'}{U} + \frac{1}{2}\frac{A'}{A} + \frac{1}{2}\frac{B'}{B} + \frac{C'}{C}\right) \tag{17}$$

Combining (15) and (17), we have

$$\left(\frac{U'}{U} + \frac{1}{2}\frac{A'}{A} + \frac{1}{2}\frac{B'}{B} + \frac{C'}{C}\right) c_s^2 = \frac{1}{2}\frac{A'}{A} + \frac{1}{2}\frac{B'U^2 + 2BUU'}{1 + BU^2} \tag{18}$$

This equation can be simplified by separating $\frac{U'}{U}$ on the left-hand side of the equation. After some algebra, we have

$$\begin{aligned}\frac{U'}{U} &= \left(-\frac{1}{2}\frac{A'}{A}(1-c_s^2) - \frac{c_s^2 B'}{2B} - \frac{c_s^2 C'}{C} + \frac{B'U^2}{2\left(1+BU^2\right)}\right) \\ &\times \left(\frac{1+BU^2}{c_s^2 + BU^2(c_s^2-1)}\right) \end{aligned} \tag{19}$$

We now define the radial four-velocity U in terms of the radial function u as follows:

$$U = -\frac{u}{\sqrt{B}\sqrt{1-u^2}} \tag{20}$$

The new function u corresponds to the four-velocity in flat Minkowsky space. It can be naturally compared to the speed of sound c_s in the accreting fluid, since both are quantities in locally flat coordinates.

From (20), the left-hand side in (19) becomes

$$\frac{U'}{U} = \frac{u'}{u(1-u^2)} - \frac{1}{2}\frac{B'}{B} \tag{21}$$

while the right-hand side simplifies to

$$\frac{U'}{U} = \frac{1}{2}\frac{A'}{A}\frac{c_s^2-1}{u^2-c_s^2} - \frac{1}{2}\frac{B'}{B} + \frac{C'}{C}\frac{c_s^2}{u^2-c_s^2} \tag{22}$$

Combining these two equations and multiplying on both sides by $c_s^2 - u^2$, we have

$$\frac{c_s^2-u^2}{1-u^2}\frac{u'}{u} = \frac{1}{2}\frac{A'}{A}\left(1-c_s^2\right) - \frac{C'}{C}c_s^2 \tag{23}$$

At the critical radius r_*, where the speed of sound in the fluid equals its flow velocity, we have $u_* = c_{s*}$. Then (23) simplifies to give

$$\frac{c_{s*}^2}{1-c_{s*}^2} = \frac{1}{2}\frac{A'}{A}\frac{C}{C'} \tag{24}$$

This is the equation we will be using in the following sections for determining the critical points.

3 Critical quantities in accretion

The critical point in the accreting fluid is the radius at which the (local) accretion velocity (in locally flat coordinates) equals the speed of sound in the fluid ($u^2 = c_s^2$). It is important to find the speed of sound and radial accretion four-velocity at the critical point as well as the critical radius itself. This information, in conjunction with the equation of state, can be used to find the parameter α in (10), which will be seen to be the parameter that determines the accretion rate.

In this section we attempt to find these quantities at the critical points for accretion onto black holes in different models. We start with the simplest case – the Schwarzschild solution – of Einstein's equations and work our way through the more exotic models.

3.1 The Schwarzschild case

In this case the line element (1) will have the form [1]

$$A(r) = 1 - \frac{r_s}{r} \tag{25}$$

$$B(r) = \left(1 - \frac{r_s}{r}\right)^{-1} \tag{26}$$

$$C(r) = r^2 \tag{27}$$

where $r_s = 2m$ in the units $G = c = 1$. r_s is known as the Schwarzschild radius, the radius of the event horizon of the Schwarzschild black hole.

From (24), substituting in for A and C we find, after calculating the derivatives and simplifying,

$$\frac{c_{s*}^2}{1 - c_{s*}^2} = \frac{r_s}{4(r_* - r_s)} \tag{28}$$

Now from (20), evaluated at the critical point, we have

$$U_*^2 = \frac{1}{B}\frac{c_{s*}^2}{1 - c_{s*}^2} \tag{29}$$

$$= \frac{r_s}{4r_*} \tag{30}$$

Using (29) to solve for c_{s*}^2, we find

$$c_{s*}^2 = \frac{U_*^2}{\frac{1}{B} + U_*^2} \tag{31}$$

$$= \frac{U_*^2}{1 - \frac{2m}{r_*} + U_*^2}$$

$$= \frac{U_*^2}{1 - 4U_*^2 + U_*^2}$$

$$\text{So} \quad c_{s*}^2 = \frac{U_*^2}{1 - 3U_*^2} \tag{32}$$

$$\text{or} \quad c_{s*}^2 = \frac{r_s}{4r_* - 3r_s} \tag{33}$$

Equations (30) and (32) correspond to those presented in [5].

Another quantity that will turn out to be important in finding the mass accretion rate onto the black hole is the critical radius r_*, which is found simply by solving for it from equation (33):

$$r_* = \frac{(1 + 3c_{s*}^2)r_s}{4c_{s*}^2} \tag{34}$$

3.2 The (extremal) Reissner-Nordström case

The Reissner-Nordström case arise when a black hole carries charge. Its line element components are [1]

$$A(r) = 1 - \frac{2m}{r} + \frac{q^2}{r^2} = \left(1 - \frac{r_+}{r}\right)\left(1 - \frac{r_-}{r}\right) \tag{35}$$

$$B(r) = \left[\left(1 - \frac{r_+}{r}\right)\left(1 - \frac{r_-}{r}\right)\right]^{-1} \tag{36}$$

$$C(r) = r^2 \tag{37}$$

This metric leads to two distinct horizons, namely

$$r_\pm = m \pm \sqrt{m^2 - q^2} \tag{38}$$

which merge in the extremal case when $q^2 = m^2$. Then

$$r_+ = r_- = m \tag{39}$$

in the appropriate units.

Following the procedure in the Schwarzschild case, by substituting for A

and C, we find for the critical speed

$$\begin{aligned} \frac{c_{s*}^2}{1-c_{s*}^2} &= \frac{r_*(r_+ + r_-) - 2r_+r_-}{4(r_* - r_+)(r_* - r_-)} \\ \Rightarrow c_{s*}^2 &= \frac{r_*(r_+ + r_-) - 2r_+r_-}{4r_*^2 - 3(r_+ + r_-)r_* + 2r_+r_-} \end{aligned} \tag{40}$$

or, in the extremal case

$$c_{s*}^2 = \frac{2r_+r_* - 2r_+^2}{4r_*^2 - 6r_+r_* + 2r_+^2} \tag{41}$$

simplifying to

$$c_{s*}^2 = \frac{r_+}{2r_* - r_+} \tag{42}$$

Also as in the Schwarzschild case, we find the critical radial four-velocity to be

$$\begin{aligned} U_*^2 &= \frac{1}{B}\frac{c_{s*}^2}{1-c_{s*}^2} \\ &= \frac{r_*(r_+ + r_-) - 2r_+r_-}{4r_*^2} \end{aligned} \tag{43}$$

and in the extremal case

$$= \frac{r_+(r_* - r_+)}{2r_*^2} \tag{44}$$

Equations (40) and (43) correspond to those given in [6].

The two cases we will investigate are $q = \frac{1}{2}m$ and $q = m$. In the first case, $r_+ = \frac{2+\sqrt{3}}{4}r_s$ and $r_- = \frac{2-\sqrt{3}}{4}r_s$. In the second case, the extremal case, $r_+ = r_- = \frac{r_s}{2}$. In these two cases then, the critical radius solves to be

$$r_* = \frac{1 + 3c_{s*}^2 + \sqrt{1 + 4c_{s*}^2 + 7c_{s*}^4}}{8c_{s*}^2} r_s \tag{45}$$

and

$$r_* = \frac{1 + c_{s*}^2}{4c_{s*}^2} r_s \tag{46}$$

respectively.

3.3 Reissner-Nordström dilatonic case

The metric in this case arises from string theory. It is one of two possible forms related by a conformal transformation. The reason we work with this

specific metric is that test particles follow geodesics when the metric is written in this form.

This type of black hole is similar to the normal Reissner-Nordström in that it is charged and has two horizons. Extra factors arise, due to a (maximal) *dilaton* coupling constant, causing additional spacetime curvature and altered geodesics for particle trajectories.

The effective four-dimensional metric that arises is [3]

$$A(r) = \left(1 - \frac{r_+}{r}\right)\left(1 - \frac{r_-}{r}\right) \tag{47}$$

$$B(r) = \left(1 - \frac{r_+}{r}\right)^{-1}\left(1 - \frac{r_-}{r}\right) \tag{48}$$

$$C(r) = r^2\left(1 - \frac{r_-}{r}\right)^2 \tag{49}$$

Here r_- and r_+ are the inner and outer horizons of the black hole, respectively.

$$r_+ = 2m \equiv r_s \tag{50}$$

$$r_- = \frac{q^2}{m} \tag{51}$$

or, in the case where $q^2 = m^2$,

$$r_- = m \tag{52}$$

It is interesting to note that in the chargeless case, the metric becomes precisely the Schwarzschild metric and the dilatonic influence on particle trajectories disappears.

After much simplification, we find that

$$c_{s*}^2 = \frac{r_*(r_- + r_+) - 2r_-r_+}{4r_*^2 + (r_- - 3r_+)r_* - 2r_-r_+} \tag{53}$$

$$U_*^2 = \frac{r_*(r_- + r_+) - 2r_-r_+}{4r_*(r_* - r_-)} \tag{54}$$

We will investigate the cases with $q = \frac{1}{2}m$ and $q = m$. In the first case $r_- = \frac{r_s}{8}$ and $r_- = \frac{r_s}{2}$ in the second case. We note that the horizons do not merge for $q = m$, as in the extremal Reissner-Nordström case. In these cases

the critical radius solves to be

$$r_* = \frac{9 + 23c_{s*}^2 + \sqrt{81 + 158c_{s*}^2 + 785c_{s*}^4}}{64c_{s*}^2} r_s \tag{55}$$

and

$$r_* = \frac{3 + 5c_{s*}^2 + \sqrt{9 - 34c_{s*}^2 + 89c_{s*}^4}}{16c_{s*}^2} r_s \tag{56}$$

respectively.

3.4 Horava-Witten braneworld case

The Horava-Witten braneworld occurs in M-theory. An extra extended spatial dimension (in addition to the nine already occurring in the usual superstring theory) makes this theory similar to the braneworld theories. Our universe lives" on a brane (a 9-dimensional spatial sheet) in the 11-dimensional bulk.

An interesting and unusual type of black hole" occurs in this theory, differing from other types of black holes in that there is no event horizon keeping the central singularity cut off from the outside.

The effective four-dimensional metric that occurs on the brane is [4]

$$A(r) = \frac{1 - \frac{2r_s}{r}}{1 - \frac{r_s}{r}} \tag{57}$$

$$B(r) = \left(1 - \frac{r_s}{r}\right)^{-1} \tag{58}$$

$$C(r) = r^2 \frac{1 - \frac{2r_s}{r}}{1 - \frac{r_s}{r}} \tag{59}$$

Following the same procedure as before we find at the critical point

$$c_{s*}^2 = \frac{r_s r_*}{4r_*^2 - 9r_s r_* + 8r_s^2} \tag{60}$$

$$U_*^2 = \frac{1}{2} \frac{r_s(r_* - r_s)}{2r_*^2 - 5r_s r_* + 4r_s^2} \tag{61}$$

In this case, the critical radius solves to be

$$r_* = \frac{1 + 9c_{s*}^2 + \sqrt{1 + 18c_{s*}^2 - 47c_{s*}^4}}{8c_{s*}^2} r_s \tag{62}$$

4 The accretion rate

The accretion rate (the rate of change of the mass of the black hole) of the fluid onto the black hole is given by [5] as

$$\dot{m} = 4\pi\alpha m^2(\rho_\infty + p(\rho_\infty)) \tag{63}$$

m being the mass of the black hole.

As will be seen, the accretion rates onto the various black hole examples mentioned in the previous section can be determined without solving for the energy density of the accretion in the different metrics. This is lucky, since the solution of the energy density in the extremal Reissner-Nordström as well as the Horava-Witten cases becomes infinite at some radius for those equations of state that are solvable. Additionally, for most equations of state the energy densities are not analytically solvable.

The accretion rate depends only on the energy density and pressure of the accretion an infinite distance from the black hole, the mass of the black hole and the parameter α. The quantity that must stay well-behaved is α, which we calculate in this section. If the accretion rate is well-behaved, it could possibly serve as a prediction for observational distinctions between the different types of black holes.

Since $\dot{m} \propto \alpha$, we will only solve for and plot α in each case. This is the distinguishing factor in the accretion rates of the different black holes. In order to compare the accretion rates, we will assume the black holes to have the same mass.

To keep the calculations simple, we will use the equation of state

$$p = \eta\rho \tag{64}$$

with $0 \leq \eta \leq 1$. Since $c_s^2 = \frac{dp}{d\rho}$,

$$c_s^2 = \eta = \text{constant} \tag{65}$$

This equation of state is physically reasonable at least in that the speed of sound remains less than the speed of light. An example is the accretion of electromagnetic radiation, for which $\eta = \frac{1}{3}$.

Once again we work our way through the different examples, after which we will compare the results.

4.1 The Schwarzschild case

By substituting in for A, B and C and evaluating equations (10) and (11) at the critical point, we obtain

$$U_* r_*^2 \exp\left[\int_{\rho_\infty}^{\rho_*} \frac{d\rho'}{\rho' + p(\rho')}\right] = \alpha \tag{66}$$

and

$$\frac{\rho_* + p(\rho_*)}{\rho_\infty + p(\rho_\infty)} \left(1 - \frac{r_s}{r_*} + U_*^2\right)^{\frac{1}{2}} = \exp\left[\int_{\rho_\infty}^{\rho_*} \frac{d\rho'}{\rho' + p(\rho')}\right] \tag{67}$$

respectively.

Evaluating the integral in the exponent:

$$\begin{aligned} & \exp\left[\int_{\rho_\infty}^{\rho_*} \frac{d\rho'}{\rho' + p(\rho')}\right] \\ = \; & \exp\left[\frac{1}{1+\eta} \int_{\rho_\infty}^{\rho_*} \frac{d\rho'}{\rho'}\right] \\ = \; & \left(\frac{\rho_*}{\rho_\infty}\right)^{\frac{1}{1+\eta}} \end{aligned} \tag{68}$$

By substituting $p = \eta\rho$, $U_*^2 = \frac{r_s}{4r_*}$ and (68) into (67), we have

$$\frac{\rho_*}{\rho_\infty} \left(1 - 4U_*^2 + U_*^2\right)^{\frac{1}{2}} = \left(\frac{\rho_*}{\rho_\infty}\right)^{\frac{1}{1+\eta}} \tag{69}$$

Using the fact that $1 - 3U_*^2 = \frac{1}{1+3c_{s*}^2}$ from [5] and using $c_{s*}^2 = \eta$, we get

$$\frac{\rho_*}{\rho_\infty} = (1+3\eta)^{\frac{1+\eta}{2\eta}} \tag{70}$$

Squaring equation (66), and substituting $U_*^2 = \frac{\eta}{1+3\eta}$, we get

$$\begin{aligned} \alpha^2 &= r_*^4 \frac{\eta}{1+3\eta} \left(\frac{\rho_*}{\rho_\infty}\right)^{\frac{2}{1+\eta}} \\ &= r_*^4 \eta (1+3\eta)^{\frac{1}{\eta}-1} \\ \Rightarrow \alpha &= \eta^{\frac{1}{2}} r_*^2 (1+3\eta)^{\frac{1-\eta}{2\eta}} \end{aligned} \tag{71}$$

Substituting the critical radius into (71) we have

$$\alpha = \frac{1}{16\eta^{\frac{3}{2}}} (1+3\eta)^{\frac{1+3\eta}{2\eta}} \tag{72}$$

Here we have chosen the scale such that $r_s = 1$.

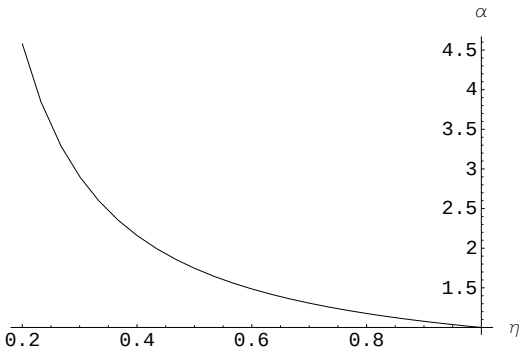

Figure 1: α plotted as a function of η in the Schwarzschild case

4.2 The Reissner-Nordström case

By substituting in for A, B and C and evaluating equations (10) at the critical point, we again obtain

$$U_* r_*^2 \exp\left[\int_{\rho_\infty}^{\rho_*} \frac{d\rho'}{\rho' + p(\rho')}\right] = \alpha \tag{73}$$

Substituting in for A, B and C at the critical point, and evaluating the integral in (11), we get

$$\left(\frac{r_*^2 - (r_+ + r_-)r_* + r_+ r_-}{r_*^2} + U_*^2\right)^{\frac{1}{2}} = \left(\frac{\rho_*}{\rho_\infty}\right)^{-\frac{\eta}{1+\eta}} \tag{74}$$

Substituting in for U_*^2 from (43), we have

$$\begin{aligned} \left(\frac{\rho_*}{\rho_\infty}\right)^{-\frac{\eta}{1+\eta}} &= \left(\frac{r_*^2 - (r_+ + r_-)r_* + r_+ r_-}{r_*^2} + \frac{r_*(r_+ + r_-) - 2r_+ r_-}{4r_*^2}\right)^{\frac{1}{2}} \\ \Rightarrow \left(\frac{\rho_*}{\rho_\infty}\right)^{\frac{2}{1+\eta}} &= \left(\frac{4r_*^2}{4r_*^2 - 3(r_+ + r_-)r_* + 2r_+ r_-}\right)^{\frac{1}{\eta}} \end{aligned} \tag{75}$$

Evaluating the square of the of (73):

$$\begin{aligned} \alpha^2 &= U_*^2 r_*^4 \left(\frac{\rho_*}{\rho_\infty}\right)^{\frac{2}{1+\eta}} \\ &= \frac{r_*^2}{4}(r_*(r_+ + r_-) - 2r_+ r_-)\left(\frac{4r_*^2}{4r_*^2 - 3(r_+ + r_-)r_* + 2r_+ r_-}\right)^{\frac{1}{\eta}} \\ &\quad \text{(substituting } \eta \text{ in)} \end{aligned}$$

$$= \frac{r_*^2}{4}(r_*(r_+ + r_-) - 2r_+r_-)\left(\frac{4r_*^2\eta}{r_*(r_+ + r_-) - 2r_+r_-}\right)^{\frac{1}{\eta}}$$

$$\Rightarrow \alpha = r_*^2\eta^{\frac{1}{2}}\left(\frac{4r_*^2\eta}{r_*(r_+ + r_-) - 2r_+r_-}\right)^{\frac{1-\eta}{2\eta}} \tag{76}$$

Substituting the values for the critical radius as well as r_+ and r_-, we find explicit expressions for α in terms of η in the various cases. Little meaning is apparent in the complicated formulae, and they are omitted. The figures for the cases $q = \frac{1}{2}m$ and $q = m$ are plotted below.

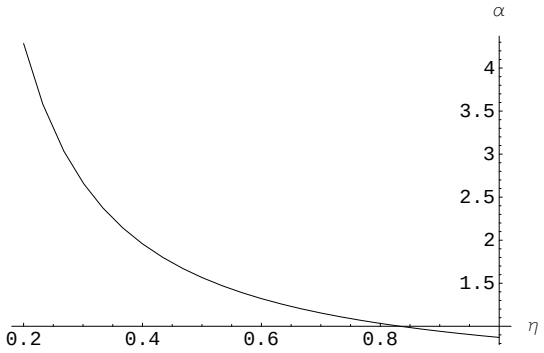

Figure 2: α vs. η in the Reissner-Nordström case with $q = \frac{1}{2}m$

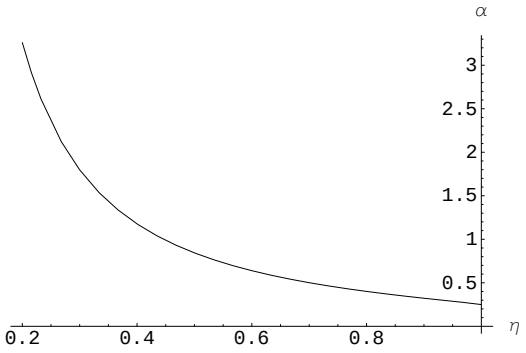

Figure 3: α vs. η in the extremal Reissner-Nordström case ($q = m$)

4.3 The Reissner-Nordström dilatonic case

Following the same steps as in the previous two subsections, we obtain from the relativistic Euler equation

$$\begin{aligned}\left(\frac{\rho_*}{\rho_\infty}\right)^{-\frac{2\eta}{1+\eta}} &= (r_*-r_-)\frac{4r_*^2+(r_--3r_+)-2r_-r_+}{4r_*^3} \\ &= \frac{1}{\eta}\frac{(r_*-r_-)[r_*(r_-+r_+)-2r_-r_+]}{4r_*^3} \end{aligned} \tag{77}$$

Squaring the continuity equation, as before, we get

$$\begin{aligned}\alpha^2 &= \frac{(r_*-r_-)^6}{r_*^2}U_*^2\left(\frac{\rho_*}{\rho_\infty}\right)^{\frac{2}{1+\eta}} \\ &= \frac{(r_*-r_-)^5[r_*(r_-+r_+)-2r_-r_+]}{4r_*^3}\left[\frac{4r_*^3}{(r_*-r_-)[r_*(r_-+r_+)-2r_-r_+]}\right]^{\frac{1}{\eta}}\end{aligned}$$

simplifying to

$$\alpha = \frac{r_*^2\eta^{\frac{1}{2}}}{\left(1-\frac{r_-}{r_*}\right)^{\frac{1-5\eta}{2\eta}}}\left[\frac{4r_*^2\eta}{r_*(r_-+r_+)-2r_-r_+]}\right]^{\frac{1-\eta}{2\eta}} \tag{78}$$

As in the above two cases, we find uninteresting expressions for α. The figures for the two cases considered are plotted below.

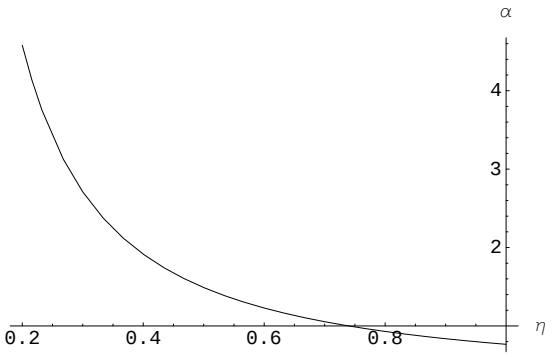

Figure 4: α vs. η in the Reissner-Nordström Dilatonic case with $q = \frac{1}{2}m$

4.4 The Horava-Witten braneworld case

Following the steps of the previous cases, we find

$$\left(\frac{\rho_*}{\rho_\infty}\right)^{\frac{2}{1+\eta}}$$

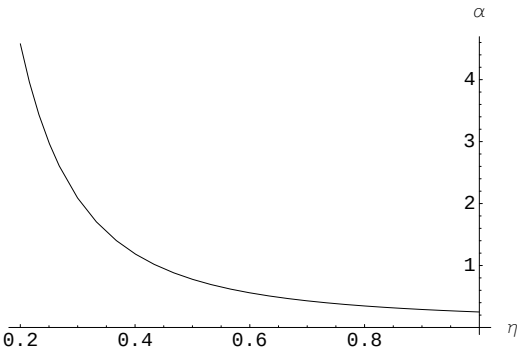

Figure 5: α vs. η in the Reissner-Nordström Dilatonic case with $q = m$

$$\begin{aligned} &= \left[\frac{2(r_* - r_s)(2r_*^2 - 5r_s r_* + 4r_s^2)}{(r_* - 2r_s)(4r_*^2 - 9r_s r_* + 8r_s^2)}\right]^{\frac{1}{\eta}} \\ &= \left[\frac{2\eta(r_* - r_s)(2r_*^2 - 5r_s r_* + 4r_s^2)}{r_* r_s (r_* - 2r_s)}\right]^{\frac{1}{\eta}} \end{aligned} \tag{79}$$

by substituting η.

By once again squaring the continuity equation and substituting in for ABC^2 and U_*^2, we have

$$\begin{aligned} \alpha^2 &= \frac{r_*^5 (r_* - 2r_s)^3}{(r_* - r_s)^3} \times \frac{1}{2} \frac{r_s(r_* - r_s)}{2r_*^2 - 5r_s r_* + 4r_s^2} \left(\frac{\rho_*}{\rho_\infty}\right)^{\frac{2}{1+\eta}} \\ &= \eta r_*^4 \frac{(r_* - 2r_s)^2}{(r_* - r_s)^2} \left[\frac{2\eta(r_* - r_s)(2r_*^2 - 5r_s r_* + 4r_s^2)}{r_* r_s (r_* - 2r_s)}\right]^{\frac{1}{\eta} - 1} \\ \Rightarrow \alpha &= \eta^{\frac{1}{2}} r_*^2 \frac{r_* - 2r_s}{r_* - r_s} \left[\frac{2\eta(r_* - r_s)(2r_*^2 - 5r_s r_* + 4r_s^2)}{r_* r_s (r_* - 2r_s)}\right]^{\frac{1-\eta}{2\eta}} \end{aligned} \tag{80}$$

Note in this case, for values of η larger than approximately $\frac{1}{3}$, α is no longer real. This may be an indication that linear equations of state aren't possible for $\eta > \frac{1}{3}$.

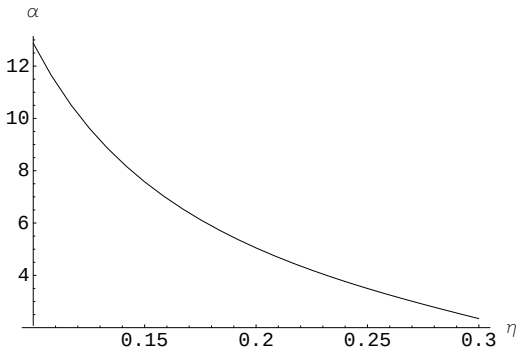

Figure 6: α vs. η in the Horava-Witten braneworld case

5 Discussion

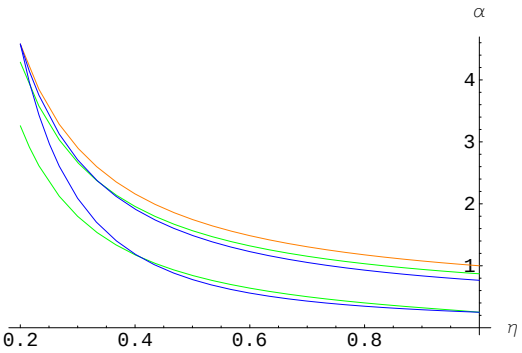

Figure 7: α vs. η for the Schwarzschild (orange), Reissner-Nordström (green) and Reissner-Nordström dilatonic (blue) cases is plotted

The first five cases of the previous section are plotted in figure (7) on the same set of axes to make it easier to draw comparisons between them. As stated in the caption, the Schwarzschild case is plotted in orange, the two Reissner-Nordström cases in green (the upper one being the $q = \frac{1}{2}m$ case and the lower one being the $q = m$ case) and the the two Reissner-Nordström dilatonic cases in blue (the upper one being the $q = \frac{1}{2}m$ case and the lower one being the $q = m$ case).

Qualitatively we find a hyperbolic dependence on η of α. We see that the Schwarzschild and the two $q = \frac{1}{2}m$ cases group together, while the two $q = \frac{1}{2}m$ cases group together at a somewhat lower value toward the right of the graph. We see that for lower values of η the two $q = m$ graphs move apart, while the top three graphs stay closely grouped.

Therefore we could potentially distinguish between the the two groups of cases observationally, possibly by the radiation emitted by the accreting fluid. At lower η we could also distinguish between the extremal Reissner-Nordström and the $q = m$ dilatonic case, as seen in the figure. The top three graphs stay together and the $q = m$ dilatonic case joins up with them to the left. Distinguishing between these cases becomes a matter of the resolving power of the measuring device. It should be remembered that the actual accretion rate $\dot{m}$ depends on the black hole mass m squared as well as the accreting fluid's energy density and pressure at infinity. If these factors are large enough, and the accretion is luminous enough, the differences between the accretion rates may well become measurable.

Regarding the charged black holes, in both the general relativity and the string theory black holes there is little difference in α from the Schwarzschild case even for the unreasonably large charge of $q = \frac{1}{2}m$. The extremal Reissner-Nordström, however, is more easily distinguished from the Schwarzschild case and is more reasonable, since it can occur in certain braneworld theories [2] without being charged at all.

In the Horava-Witten case plotted in figure (6), we also obtain a hyperbolic behaviour. It stops abruptly at a value of about $\eta = \frac{1}{3}$, where alpha is no longer well-behaved. It could be that for accretions exerting pressure per energy density greater than that of radiation, a linear relationship is not possible close to the singularity. One possible explanation for this could be a back reaction in the fluid.

6 Conclusion

In this project distinctions were made between different types of black holes by considering their respective accretion rates. This was partially achieved. It was applied to an idealised case with a perfect test-fluid accretion and an unrealistic equation of state. The charges of the black holes were exaggerated in the Reissner-Nordström and dilatonic cases to what one would expect in nature. The test-fluid assumption (that the mass of the fluid is negligible compared to the mass of the black hole) at least seems like a reasonable one in most cases. With these simplifications reasonable theoretical differences were seen in the accretion rates in some of the cases.

To make this theoretical technique more useful for the comparison with observations, the analysis should be extended to accretions with more realistic equations of state and to non-ideal fluids that could feel back reactions and strong internal forces. Extensions to rotating black holes could also be investigated. With such modifications, observations of accretion onto black holes may eventually discover the existence of more exotic objects in the universe.

7 Acknowledgements

I would like to extend my sincere gratitude to Dr. Tupper for the many hours he spent explaining the details of this project to me. Thank you for all the interesting discussions and for always being available to clarify my inevitable problems.

I would like to thank Deanne de Budé for her helpful suggestions.

Thank you to the National Institute of Theoretical Physics (NITheP) and the University of Cape Town for their financial support.

References

[1] R. d'Inverno, *Introducing Einstein's Relativity*, Oxford University Press (2007).

[2] P. McFadden, N. Turok, *Effective theory approach to brane world black holes*, Phys. Rev. D 71, 086004 (2005).

[3] R. Casadio, B. Harms, *Testing string theory via black hole space-times*, ArXiv:gr-qc/9903069v1 (1999).

[4] J. Taylor, *UCT Physics Honours Project: Black-holes in the Horava-Witten Braneworld* (2007).

[5] E. Babichev, V. Dokuchaev, Yu. Ershenko, *Black hole mass decreasing due to phantom energy accretion*, ArXiv:gr-qc/0402089v3 (2004).

[6] E. Babichev, S. Chernov, V. Dokuchaev, Yu. Ershenko, *Phantom threat to cosmic censorship*, ArXiv:0806.0916v3 [gr-qc] (2008).